

**This is an electronic reprint of the original article.  
This reprint *may differ* from the original in pagination and typographic detail.**

**Author(s):** Torgovkin, Andrii; Chaudhuri, Saumyadip; Malm, Jari; Sajavaara, Timo; Maasilta, Ilari

**Title:** Normal-Metal–Insulator–Superconductor Tunnel Junction With Atomic-Layer-Deposited Titanium Nitride as Superconductor

**Year:** 2015

**Version:**

**Please cite the original version:**

Torgovkin, A., Chaudhuri, S., Malm, J., Sajavaara, T., & Maasilta, I. (2015). Normal-Metal–Insulator–Superconductor Tunnel Junction With Atomic-Layer-Deposited Titanium Nitride as Superconductor. *IEEE Transactions on Applied Superconductivity*, 25(3), Article 1101604. <https://doi.org/10.1109/TASC.2014.2383914>

All material supplied via JYX is protected by copyright and other intellectual property rights, and duplication or sale of all or part of any of the repository collections is not permitted, except that material may be duplicated by you for your research use or educational purposes in electronic or print form. You must obtain permission for any other use. Electronic or print copies may not be offered, whether for sale or otherwise to anyone who is not an authorised user.

# Normal Metal-Insulator-Superconductor Tunnel Junction with Atomic Layer Deposited Titanium Nitride as Superconductor

Andrii Torgovkin, Saumyadip Chaudhuri, Jari Malm, Timo Sajavaara and Ilari J. Maasilta

**Abstract**— We report the fabrication of 70 - 350 nm thick, superconducting titanium nitride ( $\text{TiN}_x$ ) films using the atomic layer deposition (ALD) technique, and the subsequent fabrication of normal metal-insulator-superconductor (NIS) tunnel junction devices from the ALD films. The films were deposited on a variety of substrates: silicon, silicon nitride, sapphire and magnesium oxide. Superconductivity, with transition temperatures ( $T_C$ ) ranging from 1.35 to 1.89 K, was observed in all films. The  $T_C$  was found to depend on both the substrate type as well as film thickness.  $\text{Cu-TiO}_x\text{-TiN}_x$  normal metal-insulator-superconductor (NIS) tunnel junction devices were fabricated from the  $\text{TiN}$  film deposited on silicon, using electron beam lithography and shadow angle evaporation techniques. These devices exhibit temperature dependent current-voltage characteristics and good thermometric response from 0.1 K to slightly above  $T_C$ . Nonlinearity in the current-voltage characteristics was observed even at temperatures as high as  $5T_C$ , indicating the presence of a pseudogap in these  $\text{TiN}_x$  films.

**Index Terms**—Atomic layer deposition, tunnel junctions, superconductivity, thin film, thermometry, pseudogap.

## I. INTRODUCTION

SUPERCONDUCTING aluminum based normal metal-insulator-superconductor (NIS) tunnel junctions exhibit impressive low temperature thermometry [1,2] and solid state cooling capabilities [3-5]. Recently, some advancements in the performance of such devices were made by replacing Al with a superconductor having higher transition temperature,  $T_C$ , and hence high value of the energy gap,  $\Delta$ . NIS devices with Nb ( $T_C \sim 6$  K) [6],  $\text{NbN}_x$  ( $T_C \sim 10.8$  K) [7] and  $\text{TaN}_x$  ( $T_C \sim 4.5$  K) [8] as the superconductor were fabricated. Here, we discuss yet another nitride which exhibits superconductivity for NIS device use, titanium nitride,  $\text{TiN}_x$ .

$\text{TiN}_x$ , just like the other superconducting nitrides, has composition dependent properties, with  $T_C$  extending up to 6 K in the best case [9]. Thus, it may be an alternative for use in temperature range above that of Al. Superconducting  $\text{TiN}_x$  can

be deposited by several techniques such as reactive sputtering [10,11], atomic layer deposition (ALD) [12-14] or pulsed laser deposition [15]. For this work, we have chosen to use ALD growth, which can provide homogenous, ultrathin films.

A possible complication with the more advanced materials is the difficulty of growing a high quality tunnel barrier, something which comes naturally with Al and its good quality thermal oxide. In Refs. [6-8], good device characteristics were only obtained with  $\text{AlO}_x$  barriers grown on Al overlayers, leading to a proximity effect induced reduction of the gap. The oxidized surfaces of  $\text{NbN}$  and  $\text{TaN}$  did produce tunnel junctions, but with much larger subgap currents than with  $\text{AlO}_x$  barriers, which is detrimental to thermometry and cooling characteristics [8].

In this paper, we report the fabrication of NIS tunnel junctions from superconducting  $\text{TiN}_x$  thin films grown by atomic layer deposition. The  $T_C$  obtained for varying substrates and film thicknesses between 70 - 350 nm ranged between 1.3 - 1.9 K, somewhat lower than for ALD films in Refs. [12,13] grown using plasma-assisted ALD. Interestingly, the native oxide of the  $\text{TiN}_x$  film was used successfully as the tunnel barrier. The devices exhibited temperature dependent non-linear current-voltage characteristics suitable for thermometry, even at temperatures well beyond the measured superconducting transition temperature of the film, thereby confirming the existence of a pseudogap. The native tunnel barriers, however, seem to be too resistive for cooler applications.

## II. FILM GROWTH AND CHARACTERIZATION

$\text{TiN}_x$  films of thicknesses  $\sim 75$ , 135 and 350 nm (measured by AFM) were grown on various types of substrates using thermal atomic layer deposition (Beneq TFS-200 instrument). Titanium tetrachloride and ammonia were used as the precursor gases (in  $\text{N}_2$  flow of 250 sccm), and the growth temperature was  $400^\circ\text{C}$  for all films. The films were deposited on the following substrates: cubic (100)  $\text{MgO}$ , hexagonal r-plane sapphire ( $\text{Al}_2\text{O}_3$ ), silicon nitride ( $\sim 300$  nm thick  $\text{SiN}$  grown on top of standard silicon substrates using LPCVD) and bare silicon (with a native oxide layer). The films grown in these conditions are nitrogen rich, as the Ti:N ratio, measured from the film grown on Si and  $\text{SiN}$  substrates by time-of-flight elastic recoil detection analysis [16], was  $\sim 1:1.2$ . From the analysis, we also obtain the main impurities in the films, which were oxygen (1-2 at. %), chlorine (1-2 at. %), and

This research has been supported by Academy of Finland Project No. 260880.

A. Torgovkin, S. Chaudhuri, J. Malm and I. J. Maasilta are with Nanoscience Center, Department of Physics, University of Jyväskylä, P. O. Box 35, FIN-40014 University of Jyväskylä, Finland. email: [andrii.torgovkin@jyu.fi](mailto:andrii.torgovkin@jyu.fi), [saumyadip.chaudhuri@gmail.com](mailto:saumyadip.chaudhuri@gmail.com), [maasilta@jyu.fi](mailto:maasilta@jyu.fi)

J. Malm and T. Sajavaara are with Accelerator Laboratory, Department of Physics, University of Jyväskylä, P. O. Box 35, FIN-40014 University of Jyväskylä, Finland. email: [jari.malm@jyu.fi](mailto:jari.malm@jyu.fi), [timo.sajavaara@jyu.fi](mailto:timo.sajavaara@jyu.fi)

hydrogen ( $\sim 0.4$  at. %). We note that  $T_C$  is known to be a sensitive function of the nitrogen content at least in the nitrogen-poor TiN films [9]. More data needs to be collected on the nitrogen-rich side, but we expect that if stoichiometric conditions can be approached,  $T_C$  values will increase.

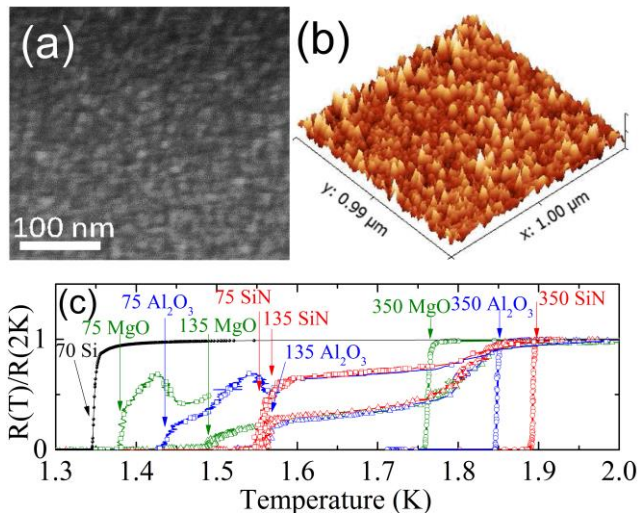


Fig. 1. Room temperature (a) scanning electron and (b) atomic force micrograph of TiN<sub>x</sub> film grown on silicon. The length scale in (a) is indicated by the horizontal bar on the bottom left. One small division of the z-scale in (b) is 4 nm. (c) Measured temperature dependence of the resistance, normalized to its value at 2 K, of TiN<sub>x</sub> films grown on different substrates. The red, blue, green and black curves correspond to SiN, Al<sub>2</sub>O<sub>3</sub>, MgO, and Si substrates respectively. The open circles, triangles, squares, and solid circles correspond to film thickness 350, 135, 75 and 70 nm. The respective arrows indicate the transition to the superconducting state.

The surface topography of the films was investigated using atomic force (AFM) and scanning electron (SEM) microscopes. The results, obtained for TiN<sub>x</sub> films on silicon, are displayed in Fig. 1 (a) and (b) respectively. AFM images reveal a smooth surface with a root mean square surface roughness  $\sim 0.8$  nm over an area of  $\sim 1\mu\text{m}^2$ . This value is less than half of what is obtained for TiN<sub>x</sub> films fabricated using pulsed laser deposition [15]. Grains of uniform size ( $\sim 10$  nm) are visible in both AFM and SEM images.

For resistivity and Hall measurements, the films were patterned using electron-beam lithography (EBL) and reactive ion etching (RIE) to obtain Hall bar geometry with a length 500  $\mu\text{m}$  and width 100  $\mu\text{m}$ . A mixture of CHF<sub>3</sub> and O<sub>2</sub> gases with flow rates 40 and 5 sccm, respectively, were used as an etchant for TiN<sub>x</sub>, while copper (50 nm thick) was used as an etch mask. The resistivity measurements were performed in a dilution fridge with a lock-in technique, using a bias current of 1  $\mu\text{A}$  at 17 Hz as the excitation in the standard four-probe configuration.

The temperature dependences of the resistances of the patterned samples on different substrates, normalized to values at 2 K, are displayed in Fig. 1(c). All films exhibited superconductivity, and depending on the substrate type and the film thickness, the transition temperature ( $T_C$ ) ranged between 1.35 and 1.89 K. For all substrates,  $T_C$  increased with film thickness, consistent with previous literature [13,14]. For a given thickness, the highest  $T_C$  was obtained for films grown

on SiN. The  $T_C$  value of films grown on sapphire was slightly lower than that of their SiN counterparts, while the lowest  $T_C$ s were obtained for films grown on MgO. The 350 nm films exhibited transition width ( $\Delta T_C$ ) of about 10 mK. Unlike the 350 nm films, the 75 and 135 nm films do not undergo an

TABLE I  
FILM PARAMETERS

Substrate	Thickness (nm)	Transition temperature (K)	Resistivity at 4.2 K ( $\mu\Omega\text{cm}$ )	Electron density $10^{22}$ 1/m <sup>3</sup>
Silicon	70	1.35	25	-
Silicon nitride	75	1.55	45	2.7
	135	1.56	970	1.6
	350	1.89	470	3.1
Magnesium oxide	75	1.38	9	2.0
	135	1.50	1850	1.3
	350	1.76	380	3.1
Sapphire	75	1.44	50	3.0
	135	1.57	990	1.5
	350	1.85	340	3.1

abrupt transition to the superconducting state. The 75 nm thick films on sapphire and MgO even exhibited a curious re-entrance-like behavior with an upturn in resistance before reaching the superconducting state. However, for reasons not yet clear to us yet, the obtained  $\Delta T_C$  of the 70 nm film grown on Si was nevertheless low,  $\sim 5$  mK. The  $T_C$  values for all the films are listed in Table 1.

For the Hall measurements, the devices were mounted on a dipstick, surrounded by a superconducting solenoid and immersed in liquid helium. The Hall and four-probe longitudinal resistances were recorded as a function of the magnetic field, using an ac resistance bridge (AVS-47). From the measurements, we determined the resistivity and the electron density, with all results listed in Table I. We see that the resistivity values have a surprisingly large range from 9  $\mu\Omega\text{cm}$  to 1850  $\mu\Omega\text{cm}$ , over two orders of magnitude. Low electron density is correlated with high resistivity, but the variation in electron density cannot explain all of the variation in resistivity (for example, for sapphire, the 75 nm and 350 nm films have approximately the same electron density, but almost an order of magnitude difference in resistivity). In recent [10,11,13,14] studies, typical TiN film resistivities have been around  $\sim 100$   $\mu\Omega\text{cm}$ . Clearly more work is required to clarify how and why resistivity can vary so much in our films. No detectable longitudinal magnetoresistance was observed in these films, for magnetic fields up to 4 T (not shown).

### III. NIS DEVICE FABRICATION AND CHARACTERISTICS

For the fabrication of the NIS devices, we used the 70 nm thick TiN<sub>x</sub> films grown on silicon, with  $T_C \sim 1.35$  K. Using EBL and RIE, TiN<sub>x</sub> pads and electrodes were first patterned. The rf power, chamber pressure and total etch time was 150

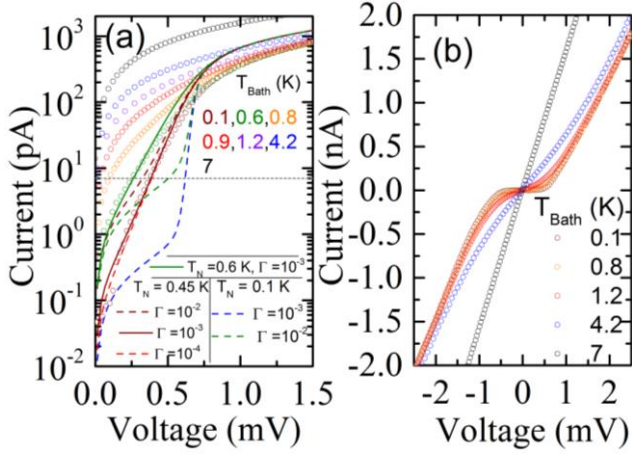


Fig. 2. Temperature dependence of the current-voltage characteristics of a double  $\text{TiN}_x\text{-TiO}_x\text{-Cu}$  junction at various bath temperatures  $T_{\text{Bath}}$  plotted in (a) log-linear and (b) linear scale (circles). The blue and green dashed lines are numerical fits assuming electron temperature  $T_N=0.1$  K, the brown lines with 0.45 K, and the green solid line with 0.6 K. The  $\Gamma/\Delta$  values used in the fits are  $10^{-3}$  for all curves except the red dashed ( $10^{-4}$ ), and the brown and green dashed ( $10^{-2}$ ). The other parameters were  $2\Delta=0.68$  meV and  $R_T=1.1$  M $\Omega$ . The horizontal dashed line in (a) represents a constant current bias of 7 pA. In (b) the non-linearity of the curve, even at 4.2 K, is clearly visible.

W, 55 mTorr, and 12 minutes, respectively. An overlay lithography was then carried out to make counter electrodes. First, the patterned  $\text{TiN}_x$  chip was oxidized, without pre-cleaning, at 400 mbar of pure  $\text{O}_2$  for 30 mins to form the tunnel barriers, after which a 100 nm thick copper (Cu) cross strip was e-beam evaporated in ultra-high vacuum, thereby forming  $\text{Cu-TiO}_x\text{-TiN}_x$  NIS tunnel junctions. The final device consisted of two such individual junctions of dimensions 20  $\mu\text{m}$  x 10  $\mu\text{m}$  and 4  $\mu\text{m}$  x 10  $\mu\text{m}$  connected in series.

The current-voltage and conductance-voltage measurements were carried out using a  $\text{He}^3\text{-He}^4$  dilution refrigerator with a base temperature of 60 mK. The measurement lines had three stages of filtering; pi-filters at 4 K, RC low-pass filters at base temperature, and finally microwave filtering between these two types of filters with the help of Thermocoax cables of length 1.5m. For the measurement of conductance characteristics, a lock-in technique with 0.04 mV excitation voltage at frequency 17 Hz was used.

In Fig. 2, the current-voltage ( $I$ - $V$ ) characteristics of the double  $\text{TiN}_x\text{-TiO}_x\text{-Cu}$  junction device, at various bath temperatures ( $T_{\text{Bath}}$ ), are shown in (a) log-linear and (b) linear scales, respectively. We tried to fit the data measured at 0.1 K using the simple theoretical model based on single-particle tunneling:

$$I = \frac{1}{eR_T} \int_{-\infty}^{\infty} d\varepsilon N_S(\varepsilon) \left[ f_N\left(\varepsilon - \frac{eV}{2}\right) - f_N\left(\varepsilon + \frac{eV}{2}\right) \right],$$

where  $R_T$  is the total tunneling resistance of the two junctions,  $f_N(\varepsilon)$  is the Fermi function in the Cu wire, and  $N_S$  is the normalized broadened superconducting quasiparticle density of states (DOS) in the Dynes model [17]

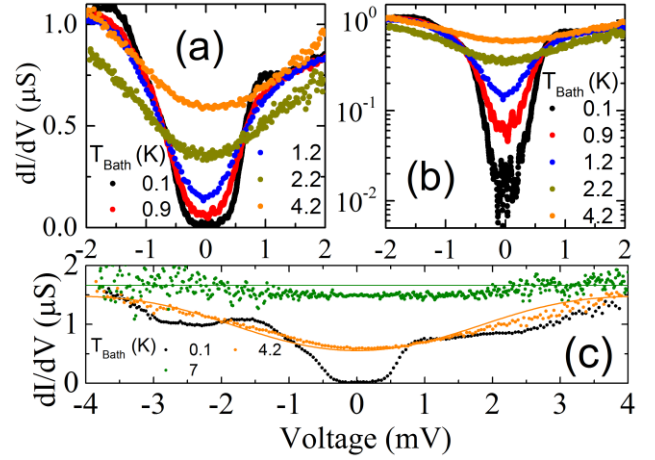


Fig. 3. Temperature dependence of conductance characteristics of a double  $\text{TiN}_x\text{-TiO}_x\text{-Cu}$  junction at various  $T_{\text{Bath}}$  plotted in (a) linear and (b) log scale. (c) Conductance characteristics for larger voltage sweep. Lines are guides to the eye (green line=constant  $dI/dV$ ).

$$N_S(\varepsilon, T_S) = \left| \text{Re} \left( \frac{\varepsilon + i\Gamma}{\sqrt{(\varepsilon + i\Gamma)^2 - \Delta^2}} \right) \right|, \text{ where } \Gamma \text{ is the parameter}$$

describing the broadening and  $\Delta$  is the superconducting gap. Unlike in our Nb, NbN or TaN devices [6-8], it was much more difficult to obtain a good theoretical fit to the data, as can be seen in Fig. 2(a), especially above the gap. However, to facilitate comparison with previous studies, we quote the parameters for the lowest temperature (0.1 K) characteristics:  $\Gamma/\Delta = 10^{-3}$ ,  $2\Delta=0.68$  meV and  $R_T=1.1$  M $\Omega$ . The fits in the subgap region ( $V < 0.5$  mV) improved clearly if the electron temperature of Cu ( $T_N$ ) was assumed to be 0.45 K instead of 0.1 K. That observation, however, should not be taken too literally due to the low quality of the fit at higher voltages  $V > 0.5$  mV. At 0.6 K, no such adjustment of effective temperature was necessary. Additionally, although our device has different individual junction dimensions (asymmetry), the deep subgap device characteristics are always independent of the asymmetry level [18] so that broadening parameter  $\Gamma$  can be estimated fairly accurately. Finally, we have also shown theoretical plots with  $\Gamma/\Delta = 10^{-2}$  for both  $T_N=0.1$  K and  $T_N=0.45$  K in Fig.2 (a). As seen, those curves clearly overestimate the deep subgap current, forcing us to conclude that the upper bound to the Dynes parameter obtained from out experimental  $I$ - $V$  plots is  $\sim 10^{-3}$ .

This level of broadening of the DOS is much below what was observed for Nb, NbN and TaN based devices [6-8]. The value for  $\Delta/k_B T_C$  is 2.9, which is much above the weak coupling BCS value of 1.76. Such a high value is in agreement with what was observed for ALD grown ultrathin TiN films in scanning tunneling (STM) experiments [19]. The specific tunneling resistance of our device, calculated by taking into account the asymmetry of the junction areas, was  $\sim 37$  M $\Omega\mu\text{m}^2$ . This value is four orders of magnitude larger than for typical  $\text{Al-AIO}_x\text{-Cu}$  junctions [8] and is much too high for any potential cooling applications.

What is interesting to note is that although the measured  $T_C$  of the  $\text{TiN}_x$  film was  $\sim 1.35$  K, the non-linearity in the  $I$ -

$V$  characteristics are visible even at  $T_{\text{Bath}} = 4.2$  K. This at least partly explains why the simple single-particle tunneling model does not work well, and indicates the presence of a pseudogap in our films. Pseudogap in ultrathin ( $\sim 5$  nm) TiN films has been observed before in STM experiments [20].

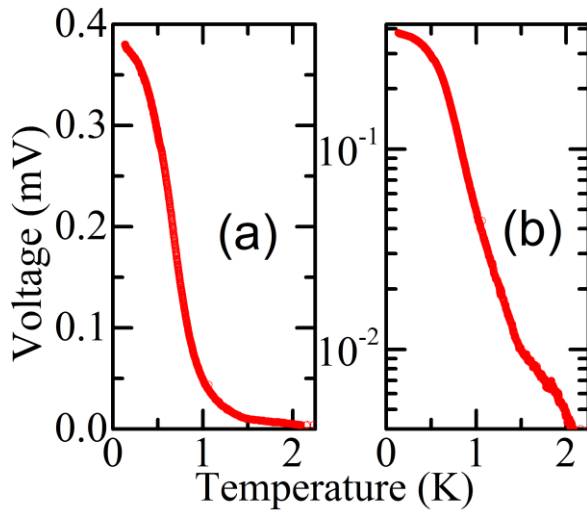


Fig. 4. Thermometry characteristics of the Cu-AlO<sub>x</sub>-Al-TiN<sub>x</sub> junction pair biased with a constant current of  $\sim 7$  pA in (a) linear and (b) log scale.

To study the pseudogap feature more, the conductance ( $dI/dV$ ) characteristics of the device at various  $T_{\text{Bath}}$  are shown in Fig. 3 in (a) linear and (b) log-scale, and on a larger voltage range in (c). The characteristics are slightly asymmetric in voltage, and not ideally BCS-like, as the DOS peak is not really observed. From the log-scale plot it is clearly seen that for  $T_{\text{Bath}} = 0.1$  K, the ratio of the zero bias conductance to the high bias conductance  $dI/dV(V = 0)/dI/dV(V \gg \Delta)$  is approximately  $10^{-2}$ , consistent with the  $I$ - $V$  data. The broad, pseudogap feature persists in the conductance characteristics even at  $T_{\text{Bath}} = 4.2$  K and 7 K, as seen in Fig. 3 (c), from we roughly estimate the characteristic pseudogap transition temperature ( $T^*$ ) to be about 7 K.

Fig. 4 shows the measured thermometric response of the device in (a) linear and (b) log-scale, respectively. The measurement was carried out in the usual configuration, whereby the device was constant current biased (7 pA), and its voltage response was measured as a function of  $T_{\text{Bath}}$ . A typical level of temperature responsivity  $\sim 0.3$  mV/K, from  $T_C$  (1.35 K) down to 0.1 K is clearly seen in (a). Even more interestingly, a smaller, but finite responsivity is still observed above  $T_C$ , more clearly from the log plot shown in Fig. 4(b). This responsivity above  $T_C$  is due to the pseudogap.

#### IV. CONCLUSIONS

In conclusion, we have fabricated superconducting TiN<sub>x</sub> films on a variety of substrates, using the atomic layer deposition technique. The deposited films exhibit good uniformity, low roughness and small grain size, making it possible to use them for the fabrication of large area devices. The superconducting transition temperature was found to

depend on the substrate type as well as the film thickness. The highest transition temperature was obtained for films grown on SiN, followed by sapphire and MgO. For a given substrate, the superconducting transition temperature increased with increasing film thickness, with the highest value 1.89 K obtained for 350 nm thick films on SiN. The resistivities of the films varied by a surprisingly large range from 9  $\mu\Omega\text{cm}$  to 1900  $\mu\Omega\text{cm}$ . More work is required to understand this variation.

We also fabricated successfully Cu-TiO<sub>x</sub>-TiN<sub>x</sub> normal metal-insulator-superconductor (NIS) tunnel junctions, using the ALD grown superconducting TiN<sub>x</sub> films and its oxide as the tunnel barrier. Good thermometric responsivity was seen in the current biased configuration, even above  $T_C$ . This surprising fact was observed to be caused by a second, pseudogap feature in the device characteristics, persisting up to a temperature of  $T^* \sim 7$  K. Most likely because of the pseudogap, the simplest single particle theory did not describe the temperature dependent current-voltage characteristics well. However, we estimated an upper bound for the broadening (Dynes) parameter to be  $\sim 10^{-3}$ , which is a good value in comparison to NIS junctions made from other complex superconducting materials. On the other hand, the specific tunneling resistance of the device was very high. If the specific resistance of the devices could be reduced, and at the same time  $T_C$  tuned a bit higher, then with the observed (or a lower value) of  $\Gamma$  high performance solid-state coolers could be realized.

#### ACKNOWLEDGMENTS

We thank J. Julin for some time of flight elastic recoil detection measurements.

#### REFERENCES

- [1] F. Giazotto, T. T. Heikkilä, A. Luukanen, A. M. Savin, and J. P. Pekola, "Opportunities for mesoscopies in thermometry and refrigeration: Physics and applications," *Rev. Mod. Phys.*, vol. 78, pp. 217-274, 2006.
- [2] M. Nahum and J. M. Martinis, "Ultrasensitive-hot-electron microbolometer," *Appl. Phys. Lett.*, vol. 63, pp. 3075-3077, 1993.
- [3] J. T. Muhonen, M. Meschke, and J. P. Pekola, "Micrometre-scale refrigerators", *Rep. Prog. Phys.*, vol. 75, 2012, Art. No. 046501.
- [4] P. J. Lowell, G. C. O'Neil, J. M. Underwood, and J. N. Ullom, "Macroscale refrigeration by nanoscale electron transport," *Appl. Phys. Lett.*, vol. 102, 2013, Art. No. 082601.
- [5] H. Q. Nguyen, T. Aref, V. J. Kauppila, M. Meschke, C. B. Winkelmann, H. Courtois, and J. P. Pekola, "Trapping hot quasi-particles in a high-power superconducting electronic cooler", *N. J. Phys.*, vol. 15, 2013, Art. No. 085013.
- [6] M. R. Nevala, S. Chaudhuri, J. Halkosaari, J. T. Karvonen, and I. J. Maasilta, "Sub-micron normal-metal/insulator/superconductor tunnel junction thermometer and cooler using Nb," *Appl. Phys. Lett.* vol. 101, 2012, Art. No. 112601.
- [7] S. Chaudhuri, M. R. Nevala, and I. J. Maasilta, "Niobium nitride-based normal metal-insulator-superconductor tunnel junction microthermometer," *Appl. Phys. Lett.*, vol. 102, 2013, Art. No. 132601.
- [8] S. Chaudhuri and I. J. Maasilta, "Superconducting tantalum nitride-based normal metal-insulator-superconductor tunnel junctions," *Appl. Phys. Lett.*, vol. 104, 2014, Art. No. 122601.
- [9] W. Spengler, R. Kaiser, A. N. Christensen, and G. Muller-Vogt, "Raman scattering, superconductivity, and phonon density of states of stoichiometric and nonstoichiometric TiN", *Phys. Rev. B*, vol. 17, pp. 1095-1101, 1978.

- [10] H. G. Leduc, B. Bumble, P. K. Day, B. H. Eom, J. Gao, S. Golwala, B. A. Mazin, S. McHugh, A. Merrill, D. C. Moore, O. Noroozian, A. D. Turner, and J. Zmuidzinas, "Titanium nitride films for ultrasensitive microresonator detectors", *Appl. Phys. Lett.* vol. 97, 2010, Art. No. 102509.
- [11] M. R. Vissers, J. Gao, D. S. Wisbey, D. A. Hite, C. C. Tsuei, A. D. Corcoles, M. Steffen, and D. P. Pappas, "Low loss superconducting titanium nitride coplanar waveguides", *Appl. Phys. Lett.* vol. 97, 2010, Art. No. 232509.
- [12] T. I. Baturina, D. R. Islamov, J. Bentner, C. Strunk, M. R. Baklanov, and A. Satta, "Superconductivity on the localization threshold and magnetic-field-tuned superconductor-insulator transition in TiN films", *Pis'ma Zh. Eksp. Teor. Fiz.*, vol. 79, pp. 416-420, 2004 (*JETP Lett.* vol. 79, pp. 337-341, 2004).
- [13] P. C. J. J. Coumou, M. R. Zuiddam, E. F. C. Driessen, P. J. de Visser, J. J. A. Baselmans, and T. M. Klapwijk, "Microwave properties of superconducting atomic-layer deposited TiN films", *IEEE Trans. Appl. Supercond.*, vol. 23, 2013, Art. No. 7500404.
- [14] E. F. C. Driessen, P. C. J. J. Coumou, R. R. Tromp, P. J. de Visser, and T. M. Klapwijk, "Strongly disordered TiN and NbTiN s-wave superconductors probed by microwave electrodynamics", *Phys. Rev. Lett.*, vol. 109, 2012, Art. No. 107003.
- [15] S. Chaudhuri, A. Torgovkin, M. Lahtinen and I. J. Maasilta, unpublished.
- [16] M. Laitinen, M. Rossi, J. Julin and T. Sajavaara, "Time-of-flight - Energy spectrometer for elemental depth profiling - Jyväskylä design", *Nucl. Instrum. Meth. Phys. Research B*, vol. 337, pp. 55-61, 2014.
- [17] R. C. Dynes, J. P. Garno, G. B. Hertel, and T. P. Orlando, "Tunneling Study of Superconductivity near the Metal-Insulator Transition," *Phys. Rev. Lett.* vol. 53, pp. 2437-2440, 1984.
- [18] S. Chaudhuri and I. J. Maasilta, "Cooling, conductance and thermometric performance of non-ideal normal metal-superconductor tunnel junction pairs", *Phys. Rev. B*, vol. 85, 2012, Art. No. 014519.
- [19] B. Sacépé, C. Chapelier, T. I. Baturina, V. M. Vinokur, M. R. Baklanov, and M. Sanquer, "Disorder-Induced Inhomogeneities of the Superconducting State Close to the Superconductor-Insulator Transition", *Phys. Rev. Lett.*, vol. 101, 2008, Art. No. 157006.
- [20] B. Sacépé, C. Chapelier, T. I. Baturina, V. M. Vinokur, M. R. Baklanov, and M. Sanquer, "Pseudogap in a thin film of a conventional superconductor," *Nat. Commun.*, vol. 1, 2010, Art. No. 140.